-

Nonlinear Decoherence in the Presence of Space Charge

(Dated: December 5, 2017)

I. INTRODUCTION

Modern hadron accelerators such as spallation sources and neutrino factories must reach higher beam intensities to meet increasingly challenging demands on performance. For example, the European Spallation Source plans for a proton beam with 5 MW average power [1]. The Proton Improvement Plan (PIP) at Fermilab [2], intended to drive neutrino experiments, will top 1 MW with the ability to expand beyond that for future upgrades. To maintain an acceptable beam loss of 1 W/m, fractional losses must be kept very low, with PIP-II requiring losses beneath 0.3% and future designs requiring many times less.

As beam power increases, its stability and lifetime may be compromised by coherent collective effects due to direct space charge – the canonical example of this is beam halo [3–6]. Other effects that can lead to beam loss in storage rings include dipole wake instabilities [7, 8] where the growth rate is proportional to the beam current; the transverse microwave instability [9] which has a threshold intensity; and the head-tail instability [10] which does not.

Each of these instabilities arise in part due to strong linear focusing driving betatron resonances at a single frequency. Head oscillations at this frequency resonantly drive the tail of the bunch in wake field driven instabilities, while transverse envelope oscillations at twice the betatron frequency in the presence of space charge produce beam halo. Introducing tune spread with amplitude can suppress these resonant interactions. If there is a transverse tune spread ΔQ, any transverse oscillations will decohere in a time $\tau \sim \Delta Q^{-1}$. For decoherence times smaller than the growth rates of the instabilities, the driving terms will damp before any beam instability can grow.

One proposed tool to mitigate these coherent instabilities is the nonlinear integrable optics [11, 12], which introduce large transverse tune spreads while still maintaining bounded, regular orbits. The principle is to construct an accelerator lattice which leads to bounded, regular motion in the transverse plane for on-momentum particles with large tune spreads. The large tune spread damps any oscillations which would normally drive coherent space charge instabilities [13]. The Integrable Optics Test Accelerator (IOTA) is being commissioned at Fermi National Laboratory for study of the concept of nonlinear integrable optics [14]. The use of a special nonlinear magnetic element introduces large tune spread with amplitude while constraining the idealized dynamics by two integrals of motion. However, integrability is susceptible to perturbations in the presence of space-charge, including tune-shift and transverse beam mismatch.

We present simulations of the IOTA ring demonstrating the viability of the nonlinear integrable optics in the presence of space charge. We first illustrate the proper procedure for creating a matched beam for the nonlinear system. We then present a lattice design scheme that corrects for perturbations arising from space-charge driven tune shift that would otherwise disrupt integrability. Lastly, we show rapid nonlinear decoherence with the appropriate choice of nonlinear magnetic field strength and beam emittance, and compare this behavior to the equivalent case with octupole inserts. These simulation results confirm mathematical models...

A. Nonlinear Integrable Optics for Single Particles

B. Impact of Space Charge

II. CREATING A MATCHED BUNCH

For a periodic accelerator matching of the bunch to the lattice usually entails finding a periodically constant set of Twiss parameters. The statistical properties of the distribution are then set equal to the Twiss parameters of the lattice. Thus matched such a bunch will remain stable in time.

For matching of a bunch to a lattice including an elliptic nonlinear element we use two versions of the lattice. The first is the base lattice without any nonlinear elements, using this lattice we can obtain the matched Twiss parameters that will be needed to construct the bunch. For the actual construction of the bunch we make use of the nonlinear potential that will be created based on the parameters of the nonlinear element. It has been found that such a matching procedure is necessary to prevent beam loss [15].

For an idealized Kapchinskij-Vladimirskij (KV) distribution all particles will have an identical value for the Hamiltonian

$$H = \frac{\hat{p}_x^2}{2} + \frac{\hat{p}_y^2}{2} + \frac{\hat{x}^2}{2} + \frac{\hat{y}^2}{2} + tU(\hat{x}, \hat{y}). \tag{1}$$

So that all particles lie on a single hyper-ellipsoid in the transverse phase space. While the KV distribution is useful due to its linear space charge forces which means that all particles experience a single tune depression it is also prone to producing numerical effects and has been

found to not produce long-term stable results in these efforts to simulate non

III. SIMULATIONS OF IOTA

A. Simulation Descriptions

Simulations of IOTA were performed with the tracking code Synergia [16]. Space charge forces were calculated using a self-consistent 2.5D model that slices the beam longitudinally and then applies transverse kicks to the bunch calculated for each slice. As we are primarily concerned with transverse effects a very long bunch $\sigma_z \gg \sigma_{x,y}$ was used with zero initial momentum spread. Under these conditions the space charge kick should be almost entirely uniform along the bunch reducing the space charge model to 2D.

The lattice elements are all modeled using first-order maps to prevent mismatch produced from higher-order effect creating a loss of integrability beyond that which will be produced by space charge. The exception to this is the nonlinear magnet which is modeled using a second order drift kick approach. The elliptic potential is a function of a strength parameter t and geometric parameter c. For invariance to be maintained these parameters must scale with the β-function as β^{-1} and $\sqrt{\beta}$ respectively along the nonlinear magnet. For construction of the physical magnet smooth scaling is not realistically achievable due to engineering constraints and the magnet is broken into 20 thin slices [**?**]. In simulation, it has been seen that 20 slices with the second order drift-kick scheme is sufficient to provide convergence. In our simulations with the inclusion of space charge we use 60 slices to ensure good convergence.

B. Adaptive matching for space charge compensation

Integrability is crucially dependent upon the $n\pi$ phase advance condition between nonlinear segments. We derived a lattice adjustment procedure to retain this condition across varying beam distributions and currents. First, a new working point for the linear lattice must be constructed to pre-empt the space charge tune shift, ΔQ. Simulations performed with sixdsimulation were used to adjust quadrupole strengths in order to offset the phase advance between the exit and entrance by the desired amount for a range of ΔQ values [17].

With the linear lattice adjusted, we then sought a beam current that provided the appropriate tune depression for the full nonlinear lattice. Because the nonlinear potential is asymmetrical, the tune shift varies in each plane as a function of the nonlinear strength t, and thus requires a nontrivial adjustment to the beam current for each configuration. To determine the operating current for a lattice, a single turn was simulated in Synergia using its explicitly linear space charge solver. Particle coordinates were sampled at the exit and entrance of the nonlinear element. Small amplitude particles were chosen such that an accurate linear normal form could be computed. A linear phase unwrap algorithm was then applied to the particles normalized coordinates and a mean phase advance in each plane was computed for the input beam current. The resulting distribution of phase advances in both planes is illustrated in Fig. 1. The optimum current is indicated by the value for which ϕ_x and ϕ_y are equally close to zero.

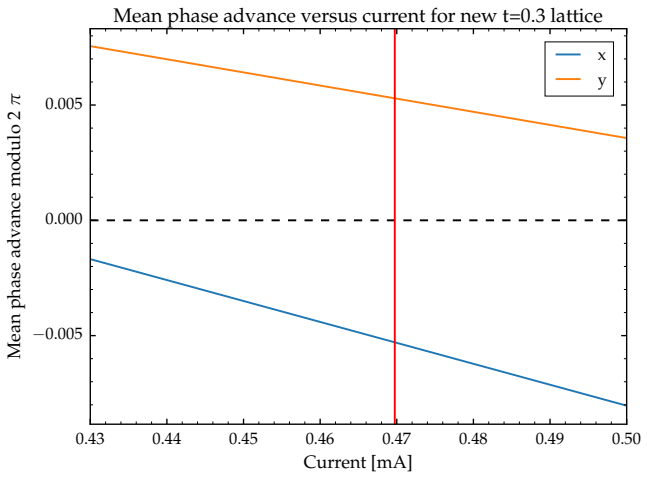

FIG. 1. The operating current for an adjusted IOTA lattice is found by minimizing the deviation in the phase advance in each plane from zero.

This procedure was repeated to construct optimized lattice and beam configurations for each combination of tune-depression and t value considered.

C. Simulation Results

To examine the operation of the nonlinear element we start the simulation with a bunch that has been matched into the elliptic potential as previous described, but after the matching procedure the bunch centroid is displaced from zero in x by 100 μm. A comparison of bunch centroid motion with and without the noninear element is shown in Fig. 2 With a purely linear lattice this displaced bunch exhibits coherent oscillations of the centroid around zero indefinitely. With the nonlinear element turned on these oscillations rapidly damp due to the tune spread created by the nonlinear magnet.

The tune spread induced for the zero current case is shown in Fig. **??**. Because the multipole expansion of the elliptic potential has a quadrupole term in the lowest order there is a splitting of the horizontal and vertical tunes, as well as the spread from the higher-order terms.

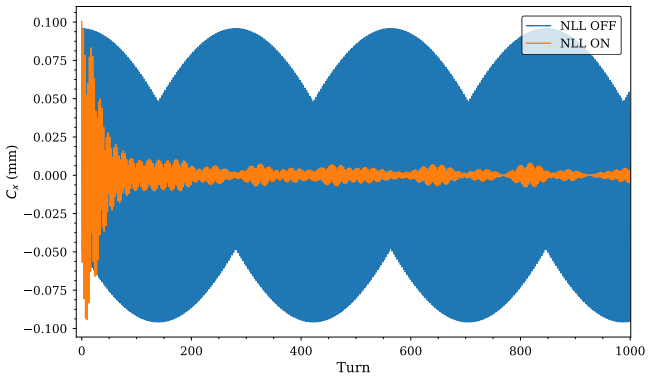

FIG. 2. Centroid (C_x) motion for a matched bunch displaced horizontally by 100 μm. Motion with the nonlinear element off is shown in blue and with nonlinear element on in orange. Space charge is not included in the simulation.

TABLE I. Characteristics of the bunch and lattice for simulations.

Quantity	Value	Units
Beam Parameters		
dQ_{SC}	0.03	-
ε_0	4, 8, 12, 16	$mm-mrad$
I	0.2056, 0.4113, 0.6169, 0.8225	mA
K	2.5	MeV
Δx	100	μm
Nonlinear Magnet Parameters		
t	0.2/0.4	-
c	0.1	$m^{1/2}$
ψ_{nll}	0.3	2π

1. *Nonlinear Decoherence with Space Charge*

We now illustrate what happens when space charge is included in the simulation. The space charge model used in Synergia was previously discussed. For all simulations with space charge a tune depression of $0.03 \times 2\pi$ / turn is maintained. For a waterbag bunch distribution an asymmetric distribution of tunes, shifted from the lattice design point, occurs. To match the beam current to the ideal tune depression as closely as possible a scan over the current is performed. The ideal current is selected to that which maximizes the number of particles in the bunch that have a phase advance from the exit to the entrance of the nonlinear element within one standard deviation of zero. Values for various emittances are shown in Table. I.

For a bunch with an initial emittance of 8 mm $-$ mrad and with a nonlinear magnet strength $t = 0.4$ the turn-to-turn centroid motion is shown in Fig. 3. It is seen that with space charge now included the damping time is greatly increased and one thousand turns is no longer sufficient to see the centroid motion decrease appreciably. The main culprit for this loss in effectiveness of nonlinear decoherence is the space charge induced tune spread. The assumption of time-invariance created by the ideal T-insert is broken for particles that do not maintain the design tune.

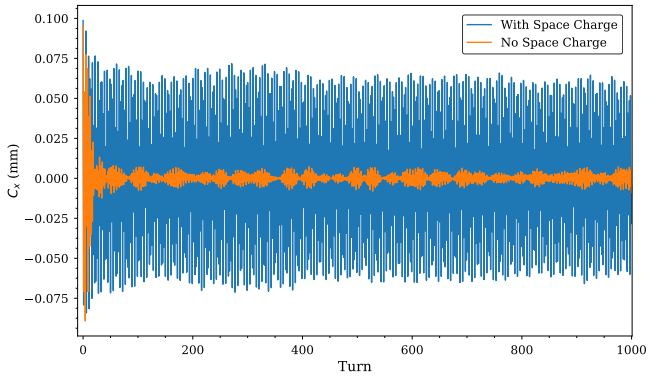

FIG. 3. Centroid (C_x) motion for a matched bunch displaced horizontally by 100 μm. Only single particle dynamics are considered for the simulation in orange. Space charge is included for the simulation shown in blue.

[1] S. Peggs *et al.*, *ESS Technical Design Report*, Tech. Rep. (European Spallation Source, 2013).
[2] V. Lebedev *et al.*, *"PIP-II Reference Design Report"*, Tech. Rep. PIP-II DocDb 1 (FNAL, 2015).
[3] J. O'Connell, T. Wangler, R. Mills, and K. Crandall, in *Proc. of Part. Accel. Conf.* (1993) p. 3657.
[4] R. L. Gluckstern, Phys. Rev. Lett. **73**, 1247 (1994).
[5] R. Jameson, *Self-Consistent Beam Halo Studies & Halo Diagnostic Development in a Continuous Linear Focusing Channel*, Tech. Rep. LA-UR-94-3753 (Los Alamos National Laboratory, 1994).
[6] D. L. Bruhwiler, in *AIP Conf. Proc.*, Vol. 377 (1995) pp. 219–233.
[7] E. D. Courant and A. M. Sessler, Rev. Sci. Instr. **37** (1966).
[8] E. Ferlenghi, C. Pellegrini, and B. Touschek, Nuovo Cimento **44**, 253 (1966).
[9] R. Talman, Nucl. Instrum. Methods **193**, 423 (1982).
[10] C. Pellegrini, Nuovo Cimento **64A**, 447 (1969).
[11] V. Danilov and S. Nagaitsev, Phys. Rev. ST – Acc. Beams **13** (2010).
[12] S. Nagaitsev, A. Valishev, and V. Danilov, in *Proceedings of HB2010*, THO1D01 (2010).
[13] S. D. Webb, D. L. Bruhwiler, D. T. Abell, A. Shishlo, V. Danilov, S. Nagaitsev, A. Valishev, K. Danilov, and J. R. Cary, "Effects of nonlinear decoherence on halo formation," (2012), arXiv:1205:7083.
[14] S. Antipov, D. Broemmelsiek, D. Bruhwiler, D. Edstrom, E. Harms, V. Lebedev, J. Leibfritz, S. Nagaitsev, C. Park, H. Piekarz, P. Piot, E. Prebys, A. Romanov,

J. Ruan, T. Sen, G. Stancari, C. Thangaraj, R. Thurman-Keup, A. Valishev, and V. Shiltsev, Journal of Instrumentation **12**, T03002 (2017).

[15] S. Webb, D. Bruhwiler, V. Danilov, R. Kishek, S. Nagaitsev, and A. Valishev, in *Proceedings, 6th International Particle Accelerator Conference (IPAC 2015): Richmond, Virginia, USA, May 3-8, 2015* (2015) p. MOPMA029.

[16] "Synergia simulation package," `https://cdcvs.fnal.gov/redmine/projects/synergia2`.

[17] A. Romanov, A. Valishev, D. Bruhwiler, N. Cook., and C. Hall, in *Proceedings of NAPAC2016*, THPOA23 (2016).